Journal of Environmental Chemical Engineering 6 (2018) 3376–3383

Contents lists available at ScienceDirect

Journal of Environmental Chemical Engineering

journal homepage: www.elsevier.com/locate/jece

Effect of structure, morphology and chemical composition of Zn-Al, Mg/Zn-Al and Cu/Zn-Al hydrotalcites on their antifungal activity against *A. niger*

Franchescoli D. Velázquez-Herrera[a], Geolar Fetter[a], Vilma Rosato[b], Andrea M. Pereyra[b,c], Elena I. Basaldella[c,*]

[a] Benemérita Universidad Autónoma de Puebla, Facultad de Ciencias Químicas, Ciudad Universitaria, 72570 Puebla, PUE, Mexico
[b] Universidad Tecnológica Nacional-Facultad Regional La Plata, 60 esq. 124, 1900, La Plata, Argentina
[c] CINDECA, CCT- La Plata-CONICET, Universidad Nacional de La Plata, 47 No, 257 (B1900AJK), La Plata, Argentina

ARTICLE INFO

Keywords:
Layered double hydroxides
Synthesis
Biocidal activity
Fungus
A. niger

ABSTRACT

Zn-Al, MgZn-Al and CuZn-Al hydrotalcites were prepared by the co-precipitation method, using the conventional hydrothermal crystallization or ultrasonic irradiation methods The samples were characterized by XRD, FT-IR and SEM, which confirmed the formation of a layered double hydroxide phase. Afterwards, the effects of composition and texture of the synthesized samples on their biocidal behavior against *A. niger* were evaluated by using traditional cultivation techniques. Among the different samples examined, hydrotalcites containing Zn, Zn-Mg and Zn-Cu showed an inhibitory effect on *A. niger* growth. Samples synthesized by the conventional method showed a greater inhibitory capacity than those synthesized by ultrasonication, but their biocidal activity was mainly determined by the presence of biocidal cations. The biocidal characteristics of zinc and/or copper in conjunction with the alkalinity of these materials were favorable for preventing fungal spread. The ZnAl hydrotalcite, the more eco-friendly material of the analyzed series, showed a good biocide performance, while the best antifungal behavior was observed for copper-containing hydrotalcites.

1. Introduction

Recent epidemiological studies have shown that pathogenic fungal microorganisms such as those of the genus *Aspergillus* have significantly increased their resistance to the fungicides currently available. This fungus can be adsorbed by animals through the skin, ingestion or inhalation and can cause aspergillosis in humans [1]. Among the *Aspergillus* fungi, the most common is *Aspergillus niger*, which can cause health problems including allergies and asthma, especially during prolonged indoor exposure. It is frequently found in fruits and vegetables, causing a disease called black mold. Also, this fungus appears on the painted surfaces of buildings producing degradation, flaking and spalling of the coating [2]. It is a very resistant fungus that grows in a wide range of temperatures, pH values, salt concentrations and humidity levels [3]. Thus, it will be interesting to find an antifungal agent that could be easily added to paints to prevent damage by fungi.

The typical antifungal agents, such as azoles or allylamines, act against fungi inhibiting the protein, cell wall and microtubule biosynthesis or disrupting the membrane and other fungal components [4,5]. Antifungal agents have also been supported on inorganic solids or in alginate pellets to form hybrid materials having a controlled release of the organic fungicides [6–14]. In some cases, the inorganic solids exhibit antimicrobial properties, due, in part, to their high surface areas that provide a good contact with microorganisms and, in others, to their chemical composition [15]. Pereyra et al. [16], reported that Ag^{+} and Zn^{2+} ions supported on A-type zeolite presented higher activity against *Aspergillus niger* when compared to traditional organic biocides [16]. An effective fungicide composed of ZnO nano-particles against *B. cinerea* and *P. expansum* was reported by He et al. [17]. Among inorganic supports, the most suitable inorganic solids could be clays, taking into account that they are chemically stable, easy to handle, nontoxic to humans and environmentally friendly [18]. Among clays, the anionic type, known as hydrotalcite, has presented high activity against various bacteria or fungi, which can be attributed to metallic ions or hydroxides liberated from the structure to the microorganism medium [10,19]. Hydrotalcites are natural or synthetic clays made up of positively charged layers balanced by hydrated anions. The general chemical formula is $[M^{2+}_{(1-x)}\ M^{3+}_{x}\ (OH)_2](X^{m-}_{(x/m)})\cdot nH_2O$, where M^{2+} and M^{3+} are divalent and trivalent metals, respectively. X^{m-} is a compensating anion with charge m-; x represents the metal ratio $M^{3+}/(M^{3+}+M^{2+})$ and *n* is the number of water molecules. Frequently, M^{2+} is a magnesium cation but it can be replaced by copper or zinc cations, which are

* Corresponding author.
E-mail address: eib@quimica.unlp.edu.ar (E.I. Basaldella).

https://doi.org/10.1016/j.jece.2018.04.069
Received 11 January 2018; Received in revised form 17 April 2018; Accepted 29 April 2018

ions that have high antimicrobial properties [18,20]. It is known that the chemical composition as well as the textural properties of hydrotalcites could be tailored by selecting the crystallization methodology and the starting mixture composition employed for their synthesis [21]. Therefore, the chemical composition, particle size and porosity of hydrotalcite materials possessing selected properties can be tailored to be included in the paint formulations to prevent fungal dissemination in houses and buildings.

In this work, the synthesis of hydrotalcites containing Mg, Zn and/or Cu with Al was carried out by the co-precipitation method followed by a crystallization process that was performed by conventional heating or by applying ultrasonic irradiation. Thus, the effect of composition, structure and textural properties of the samples can be considered when employed as fungicidal against *A. niger*. The microbiological evaluation was performed using traditional cultivation techniques.

2. Materials and methods

2.1. Materials

Magnesium (Sigma-Aldrich, 99%), copper (Sigma-Aldrich, 98%), zinc (Sigma-Aldrich, 98%) and aluminum nitrate (Sigma-Aldrich, 98%) were used as reactants to synthesize the hydrotalcites. Ammonium hydroxide (Baker, 28%) was used as precipitating agent.

2.2. Material syntheses

Zn-Al, MgZn-Al and CuZn-Al hydrotalcites with a molar ratio of M^{2+}:M^{3+} equal to 2:1 were synthesized. Depending on the desired hydrotalcite product, 1.5 mol L^{-1} solutions of $Al(NO_3)_3{\cdot}9H_2O$, $Zn(NO_3)_3{\cdot}9H_2O$ and/or $Cu(NO_3)_2$ and/or $Mg(NO_3)_3{\cdot}9H_2O$ were prepared. NH_4OH solution (1.5 mol L^{-1}) was used as precipitating agent.

For conducting the hydrotalcite crystallization process, two different methods were used: ultrasonic irradiation and conventional hydrothermal heating.

2.2.1. Ultrasonic hydrotalcite syntheses (U series)

Each sample was prepared by simultaneously dropping an aqueous solution of the corresponding metal nitrates and an ammonium hydroxide solution. The dropping flow of each solution was adjusted to maintain a constant pH of 8.0. The hydrotalcites synthesized at constant pH result in solids were the composition results more homogeneous than those synthesized at variable pH [22]. The resulting mixture was subjected to crystallization for 20 min in an ultrasonic cleaner bath (Branson 5510, 135 W, 42 kHz). Then, the solid was recovered, washed with distilled water and allowed to precipitate for 24 h. Finally, the decanted solid was separated from the liquid, washed with distilled water to achieve a constant pH of the wastewater *ca.* to 7.6, and dried in an oven at 70 °C for 24 h.

2.2.2. Hydrotalcites obtained by conventional hydrothermal synthesis (C series)

The synthesis mixture was obtained following the aforementioned simultaneous dropping method. The resulting mixture was conventionally treated at 80 °C for 24 h, under stirring. At the end of the synthesis, the solid fraction was recovered and treated as was described above. The cations incorporated in the starting crystallization mixtures for obtaining the different hydrotalcite samples are detailed in Table 1.

2.3. Characterization methods

2.3.1. X-ray diffraction (XRD)

A Bruker D8 Discover diffractometer coupled to a copper anode (λ = 1.54056 Å) X-ray tube and equipped with a Göbel mirror was used to obtain the X-ray diffraction patterns. Diffraction data were collected at room temperature in the Bragg-Brentano θ–2θ geometry. The scanning covered the 5°–70° range with a step angle of 0.025° and an integration time of 36 s. Crystallite sizes were obtained from the XRD data agreeing to the Debye-Scherrer equation: $d = 0.9\ \lambda/(B \cos \theta)$, where d, λ, B and θ signify the crystallite size, Cu Kα wavelength (0.15428 nm), full width at half-maximum intensity (FWHM) of the reflection in radians, and Bragg's diffraction angle, respectively [23].

Table 1
Sample identification, M^{2+} and M^{3+} cations present in the starting mixture and the nominal M^{2+}/Al molar ratios.

Sample	M^{2+} cations incorporated	M^{3+} cation	Molar ratio (M^{2+}:Al)	Crystallization method
UZA	Zn	Al	2:1	Ultrasonication
UZMA	Zn, Mg	Al	2:1	Ultrasonication
UZCA	Zn, Cu	Al	2:1	Ultrasonication
CZA	Zn	Al	2:1	Conventional hydrothermal
CZMA	Zn, Mg	Al	2:1	Conventional hydrothermal
CZCA	Zn, Cu	Al	2:1	Conventional hydrothermal

2.3.2. Fourier transform infrared (FTIR) spectroscopy

FTIR spectra in the region of 4000–400 cm^{-1} were recorded with a Magna-IR Spectrometer 550 Nicolet. The sample was dispersed in KBr pellets

2.3.3. Scanning electron microscopy (SEM)

Particle size and morphology were observed by SEM, by means of a Philips 505 microscope. The samples were covered with gold prior to analysis to avoid charging effects. The local elemental chemical composition was determined by energy-dispersive spectroscopy (EDS).

2.3.4. Inductively coupled plasma-Optical emission spectrometer (ICP-OES)

Al, Mg, Cu and Zn contents were measured by ICP-OES. The samples (*ca.* 1 mg), were dissolved in a HNO_3 solution before analysis with a Varian 730-ES equipment.

2.3.5. Fungus and antimicrobial assay

Aspergillus niger fungus was selected to evaluate the antimicrobial activity of synthesized hydrotalcites. The *A. niger* strain used for these studies was isolated from a painted wall of the San Francisco de Asis Church, La Plata, Argentina (registered as No. LPSc 1153 at the Instituto Spegazzini, Argentina) [24].

The fungus was aerobically grown for 10 days at 30 °C in an agar maltose-peptone (AGMS) medium (agar 20 g (Britania), maltose 30 g (Biopack) and meat peptone 5 g (Britania) in 1000 mL of distilled water. Then, an aliquot of this culture was aseptically transferred to an Erlenmeyer flask with sterile distilled water, and the *A. niger* suspension was appropriately diluted (0.3×10^6 spores mL^{-1}). The number of spores was estimated in a Neubauer chamber. Due to the small size of *A. niger* spores (3–4 μm in diameter), the count was obtained using the smallest grids at the greatest magnification.

In the general procedure, each synthesized hydrotalcite was distributed in sterile Petri dishes containing AGMS medium (10 mL). The C series (CZA, CZMA and CZCA samples) was tested first, followed by the U series (UZA, UZMA and UZCA samples). The growth of each series was compared to its own three control plates (without hydrotalcites). For each synthesized hydrotalcite, different weights were added to the Petri dishes in order to prepare samples containing increasing Zn concentrations: 20, 40, 80, 100 and 120 mgm L^{-1} of Zn^{2+}. This methodology allowed us to analyze whether the replacement of Zn^{2+} by another ion (Mg^{2+} or Cu^{2+}) produces a synergistic effect or reduces the antifungal capacity of hydrotalcites.

With the aim of evaluating the capability of the fungus to spread from the site of colonization, inoculum was applied in a single point in

Table 2
Elemental composition (in wt%) obtained by EDX and ICP-OES and the resulting metallic molar ratio of the hydrotalcite samples.

Sample	EDX					ICP-OES				
	Al	Mg	Zn	Cu	M2+/Al molar ratio	Al	Mg	Zn	Cu	M2+/Al molar ratio
UZA	9.4	0.0	36.6	0.0	1.6	10.1	0.0	43.3	0.0	1.8
UZMA	12.1	5.4	26.5	0.0	1.4	10.1	5.6	21.7	0.0	1.5
UZCA	9.5	0.0	25.1	19.1	1.9	9.1	0.0	17.7	15.0	1.5
CZA	8.5	0.0	44.4	0.0	2.1	7.8	0.0	31.3	0.0	1.7
CZMA	11.0	4.9	33.3	0.0	1.7	11.1	6.0	22.8	0.0	1.4
CZCA	8.5	0.0	25.9	20.4	2.4	10.0	0.0	21.1	19.8	1.7

the center of the Petri dishes. After 5 days, the average area of *A. niger* colonies (cm^2) and percentage of colonized area (%) were measured using the grid.

All tests were done in triplicate.

3. Results and discussion

3.1. Chemical composition of the synthesized hydrotalcites

The EDX elemental composition (Table 2) shows that the M^{2+}/Al molar ratios of the U series (1.6, 1.4 and 1.9) are lower than the nominal value of 2, indicating that the ultrasonic irradiation favors the diffusion of Al^{3+} ions to the core of the hydrotalcite particles. This phenomenon was already reported for hydrotalcites synthesized with microwave irradiation [25]. For the C series, the molar ratios are slightly higher than the nominal value of 2, except for the trimetallic hydrotalcite, CZMA sample, with a value of 1.7. It can also be observed that for samples containing zinc and aluminum or those containing zinc, copper and aluminum, the metallic ratios are very close to the nominal value, *i.e.*, the nature of the metallic cation affects the M^{2+}/Al molar ratio to a lesser extent. Furthermore, due to the easy incorporation of copper ions in the hydrotalcite network [19], the molar ratios of the UZCA and CZCA samples had the highest value for each sample of the series. Nevertheless, it is well known that EDX provides only a semiquantitative chemical analysis determination, an influence of the chemical inhomogeneity of the sample area selected for inspection being also expected. Thus, to obtain a more accurate elemental composition, the samples were analyzed by ICP-OES. The resulting metallic molar ratio values for UZA and UZMA samples were slightly higher than those obtained by EDX, while the UZCA sample presented a molar ratio value of 1.5, which was slightly lower. For samples treated by the conventional method, the molar ratios, in all cases, presented lower values of 1.7, 1.4 and 1.7 for samples CZA, CZMA and CZCA, respectively, confirming that the Al^{3+} ions diffuse more than the M2+ cations into the hydrotalcite particle core. Furthermore, the conventional method also contributes to the Al^{3+} diffusion. Thus, the hydrotalcite composition depends on the type of thermal treatment used for the crystallization step as well as on the nature of the cation incorporated.

3.2. Crystallinity and structural features

The XRD patterns of the samples obtained by the ultrasonication and conventional treatments are shown in Fig. 1.

Hydrotalcites showed characteristic peaks corresponding to the crystallographic planes (003), (006), (009), (012), (110) and (113) [21]. These peaks were identified according to the JCPDS card 00-014-0191, ascribed to carbonated Mg-Al hydrotalcite. In all cases, no impurities were detected.

In general, the hydrotalcites synthesized by ultrasonication (U series, Fig. 1a) showed reflection peaks with higher intensity than those obtained by conventional synthesis. This result is in agreement with those reported in previous work [26]. Likewise, the (110) and (113) crystallographic planes were present as a single wide peak, indicating a high degree of disruption of elements in the crystalline lattice [27]. The lower crystallinity observed for sample UZCA, compared to the values corresponding to UZA and UZMA, could be attributed to the crystalline lattice distortion in the hydrotalcite framework produced by the presence of copper [28,29]. The broadening of the (00l) peaks may also be attributed to the small particle sizes of the copper-containing hydrotalcite caused by the Jahn-Teller effect [18]. The incorporation of Cu^{2+} ions could also be affected by the presence of NH_4^+ [30].

According to the results obtained in the X-ray diffraction patterns of the conventionally synthesized hydrotalcites, CZA and CZMA showed a double peak in the planes (003) and (006), which can be attributed to the double symmetry in the structure. These sections of different symmetry were generated during the crystallization process due to random sheet stacking [31].

The X-ray diffraction pattern of CZCA presented a single peak corresponding to (110) and (113) crystallographic planes, which is attributed to a high degree of disarrangement of the metallic elements in the hydrotalcite crystalline network [18] due to the fact that copper promotes a disorder in the hydrotalcite lattice, as mentioned before. On the contrary, the separation of these peaks in the samples without copper (CZA and CZMA) suggests a better accommodation of the metallic ions in the crystalline network when the crystallization proceeds via the conventional hydrothermal synthesis.

Structural parameters of the hydrotalcites are shown in Table 3. The diffraction peaks were indexed to a hexagonal lattice with rhombohedral 3R symmetry. It is known that the parameter a ($a = 2 \times d_{110}$) varies according to the metal – metal distance within the layers, and the parameter c ($c = 3 \times d_{003}$) depends on the metal cation nature, the water content and the size of the charge-compensating anions present in the interlayer region [32]. For the prepared samples, the values of the lattice parameter a are almost constant, $a \approx 3.06$ Å, revealing that the average intermetallic spaces of the obtained layered matrices are identical. Additionally, the interlayer distance, d_{003} parameter, is ≈8.8 Å, indicating that NO_3^- ions are present in the interlayer space [22]. For CZA and CZMA samples, a segregated phase with parameters $a \approx 3.06$ and $d_{003}^* \approx 7.7$ Å, which correspond to carbonated hydrotalcite [22], was also obtained.

In the U series, the c parameter value (26.6 Å) is the same for UZA and UZMA, diminishing to 26.1 for UZCA. Similar results are obtained for the C series, where the c value diminishes from 26.5 to 26.1 Å. The decrease in c values indicates that the presence of copper influences the space between the anionic clay layers.

The crystallite sizes of the samples were determined by the Scherrer equation and reported in Table 3. The samples prepared with ultrasound irradiation presented crystallite sizes from 6 to 31 nm, while those prepared by the conventional method ranged from 5 to 14 nm. The ultrasound promotes the formation of bigger crystallites than the conventional method. Furthermore, it can be seen that the hydrotalcites containing copper are composed of smaller particles than those observed in Zn or Zn/Mg hydrotalcites. Copper incorporation produces a distortion of the hydrotalcite network along with a reduction in the crystallite sizes. Hence, the particle size depends on the methodology used for the crystallization and on the hydrotalcite composition.

3.3. Functional groups

The FTIR spectra of the hydrotalcites obtained by ultrasonication and conventional methods are shown in Fig. 2.

Similar FTIR spectra are observed for all synthesized hydrotalcites. Bands corresponding to OH group vibrations are present at 3500 cm^{-1}, being mainly attributed to the hydroxyl groups of the hydrotalcite layers, interlaminar water molecules, and to OH and NH_4^+ stretchings. The 1650 cm^{-1} bands are assigned to the water confined between hydrotalcite layers [33]. The band at 2400 cm^{-1} is assigned to the carbon

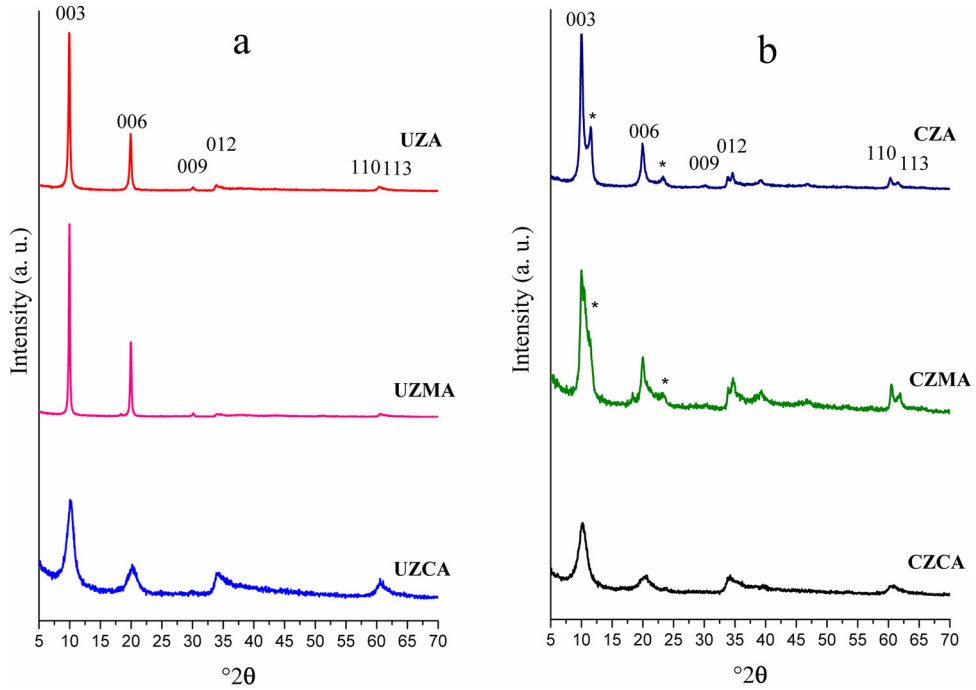

Fig. 1. X-ray diffraction patterns of the samples obtained by a) ultrasonication (UZA, UZMA and UZCA) and b) conventional (CZA, CZMA and CZCA) methods. *Secondary hydrotalcite phase.

Table 3
Structural parameters of synthesized hydrotalcites.

Sample	A (Å)	c (Å)	d_{003} (Å)	c* (Å)	d_{003}* (Å)	Crystallite size (nm)	Specific surface area (m^2/g)
UZA	3.05	26.6	8.8			26	0.3
UZMA	3.05	26.6	8.8			31	0.7
UZCA	3.05	26.1	8.7			6	4.1
CZA	3.07	26.5	8.8	23.0	7.7	14	2.0
CZMA	3.06	26.5	8.8	23.1	7.7	13	13.0
CZCA	3.06	26.1	8.7			5	14.4

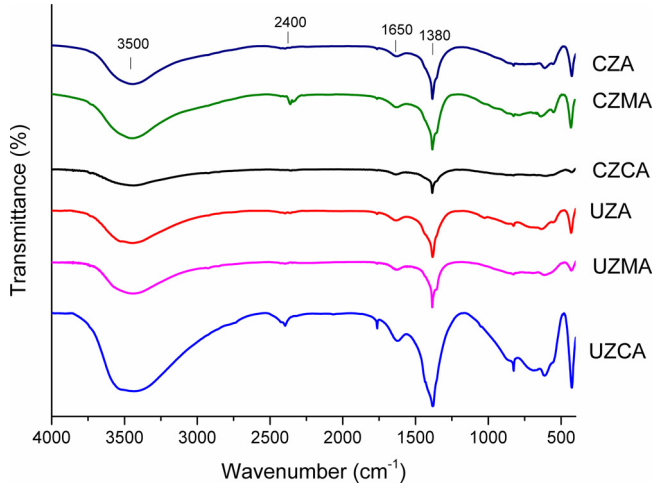

Fig. 2. FTIR spectra of hydrotalcites synthesized by ultrasonication (UZA, UZMA and UZCA) and conventional (CZA, CZMA and CZCA) methods.

dioxide from the laboratory atmosphere and it does not correspond to a compound present in the samples. Vibrations located at 1380 cm^{-1} are associated with interlayered nitrates (NO_3^-). Bands appearing between 400 and 900 cm^{-1} are related to the presence of M^{2+} and M^{3+} cations [30,34].

3.4. Morphological and textural properties

The SEM images of the synthesized hydrotalcites are shown in Fig. 3. The ZnAl and ZnMgAl samples, independently of the synthesis method, presented the usual reported morphologies ascribed to hydrotalcites, consisting of irregular and stacked flakes [35] forming heterogeneous chunks with a rather smooth surface. Furthermore, for the samples synthesized by the conventional method the combination Zn and Mg promoted a house of cards arrangement of the lamellae. If copper was present, agglomerates were composed of small particles in the case of the sample prepared by ultrasonication, while a mixture of small particles with well-defined crystals in the form of spikes can be clearly seen in the sample conventionally prepared [36]. In the case of copper-containing samples, the formation of smaller hydrotalcite particles was observed.

Table 3 compares the specific surface area of the samples. For samples treated with ultrasound, the UZA sample presented the lowest surface of 0.3 m^2/g and it increased to 0.7 m^2/g when magnesium is added, but a much higher value 0f 4.0 m^2/g is found when magnesium is changed by copper. For samples prepared conventionally, the surface areas increased much more, achieving a value of 14.4 m^2/g for the sample containing copper. If the morphology is considered, the surface areas are in accordance, and it is clear that the samples where the arrangement was more ordered in stacked flakes, the areas were lower than those where the arrangement was more irregular, as in house of cards or with crystals in the form of spikes, resulting in solids with higher surface areas.

3.5. Microbiological assays

The average area of *Aspergillus niger* colonies (cm^2) and percentage of colonized area (%) obtained for the different prepared samples are listed in Table 4. The standard deviation values corresponding to the results obtained in the microbiological tests varied between 0 and 1.7. As mentioned, each row shows the test results for samples containing equivalent Zn weights.

As can be seen in Table 4, all hydrotalcites exerted an inhibitory

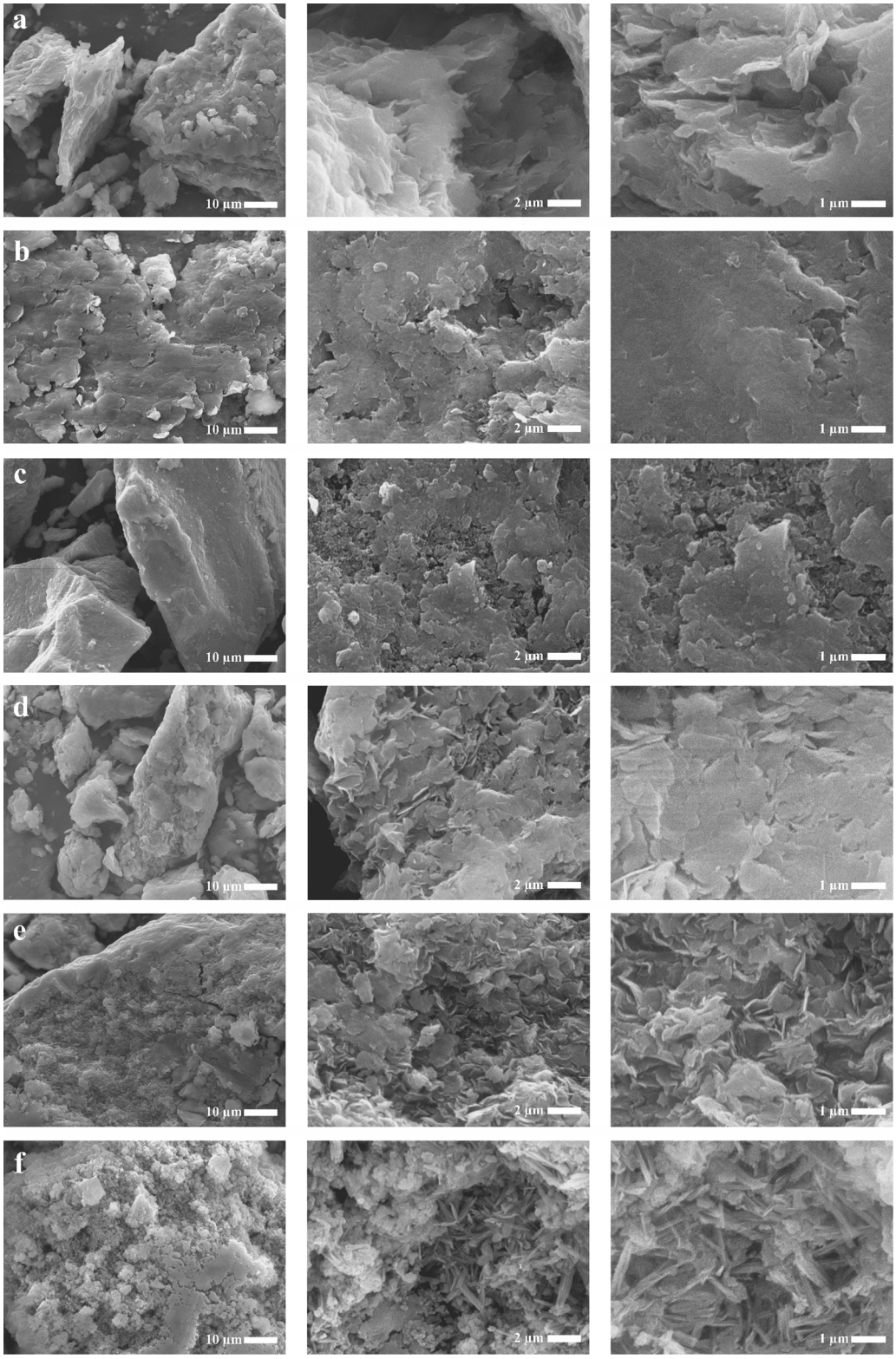

Fig. 3. SEM images of hydrotalcites synthesized by ultrasonication: a) UZA, b) UZMA, c) UZCA samples, and conventionally: d) CZA, e) CZMA, f) CZCA samples. Magnifications are presented in increasing order from left to right at 1000, 5000 and 10000 X.

effect on the growth of *A. niger*. Each row corresponds to samples having equal weight of Zn^{+2}. By comparing the results obtained in both series for samples containing equivalent weights of Zn^{2+}, hydrotalcites synthesized by the conventional method (C series) showed a greater inhibitory capacity than those synthesized by ultrasonication (U series). The better antifungal activity of the hydrotalcites synthesized by the conventional method could be attributed to the smaller crystallite sizes of the C samples, where a better contact with the fungus were expected. In addition, the morphology of the CZCA sample, characterized by a mixture of small particles with well-defined crystals in the form of spikes could favor the contact with fungus, and then, increasing its antimicrobial activity. Also, this can be supported by the surface area of

Table 4
Aspergillus niger culture growth at 120 h. Average of three measurements.

mg Zn.mL^{-1}	Average area of *A. niger* colonies, (cm^2)						Percentage of colonized area, (%)					
	UZA	UZMA	UZCA	CZA	CZMA	CZCA	UZA	UZMA	UZCA	CZA	CZMA	CZCA
Control	30.00			34.50			52.50			60.80		
20	3.80	24.00	1.07	3.20	13.75	0	6.65	42.29	1.89	5.6	24.23	0
40	2.24	22.05	0	1.85	12.75	0	3.92	39.4	0	3.24	22.47	0
60	1.05	20.20	0	1.20	10.90	0	1.84	35.35	0	2.11	19.75	0
80	0.28	17.50	0	0	8.75	0	0.49	30.2	0	0	15.31	0
100	0	11.50	0	0	6.20	0	0	19.8	0	0	10.85	0
120	0	10.98	0	0	3.90	0	0	19.22	0	0	6.88	0

this sample which presented the higher value of 14.4 m^2/g. The average area of *A. niger* colonies and the percentage of colonized area for the C series are significantly lower than for the U series. It is also important to note that the growth of *A. niger* on the control plate corresponding to the C series (34 cm^2 of colonized area or 60.80% of Petri dish coverage) was higher than that observed in the U control plate (30.00 cm^2 of colonized area or 52.50% of Petri dish coverage).

The images of microbiological tests performed to determine the average area of A. niger colonies (cm^2) and percentage of colonized area (%) for U and C series are shown in Figs. 4 and 5, respectively. It is evident that the C series demonstrated the greatest ability to inhibit the growth and sporulation of the fungus.

With regard to the composition, Zn/Al hydrotalcites (Table 4, UZA and CZA samples) showed strong inhibitory capacity against the fungal strain. For the lowest zinc concentration used in the microbiological test (20 mgm L^{-1}), a noteworthy reduction in colonized area of 87.3% for UZA and 90.8% for CZA was reached with respect to the control plate. Thus, UZA and CZA hydrotalcites demonstrated to be very effective in the control of *A. niger* growth even at a low zinc content. The minimum inhibitory concentration (MIC) value or completed inhibition was reached in hydrotalcites that contain above 80 mgm L^{-1} of zinc. Figs. 4b and 5b show fungal growth in UZA and CZA samples respectively before reaching the complete inhibition of *A. niger* growth.

Hydrotalcites containing zinc-magnesium (UZMA and CZMA samples) exhibited the lowest biocidal capacity. For these samples, there was no complete inhibition of *A. niger* growth even at the maximum concentrations tested (equivalent weight of hydrotalcite containing 120 mg Zn.mL^{-1}). The UZMA sample showed the minimum biocidal capacity. According to the value shown in Table 4 obtained from the microbiological test (Fig. 4c) for UZMA sample, 120 mg Zn.mL^{-1} produced only a 63.4% reduction in the colonized area with respect to the control plate. The inhibition results for CZMA were more positive than for UZMA sample. CZMA showed a decrease of 88.7% in the colonized area using the equivalent weight of hydrotalcite containing 120 mg Zn.mL-1 (Table 4 and Fig. 5c). Certainly, the presence of magnesium contributed to counteracting the inhibitory capacity of zinc, since magnesium is essential for the growth of fungi. It is widely known that magnesium is part of the synthesis of amino acids, nucleic acids and ATP, and participates as cofactor in various enzymatic reactions, among many other functions [37].

Copper-containing hydrotalcites (UZCA and CZCA samples) had the best inhibitory effect (Figs. 4d and 5d). As can be seen in Table 4, concentrations of 20.00 mg mL^{-1} of Zn – 15.21 mg mL^{-1} of Cu in CZCA hydrotalcites were enough to completely inhibit the growth and sporulation of *A. niger*. Microbiological tests performed for CZCA at concentrations lower than 20 mg mL^{-1} showed that from 15 mg mL^{-1} of zinc there was no evidence of fungus growth or sporulation. Then, this concentration could be defined as MIC. In the UZCA test, a slightly higher concentration of metals was required to achieve complete inhibition since for hydrotalcites containing 20 mg mL^{-1} of Zn^{2+}, some colonies covered an area of 1.07 cm^2 (Table 4 and Fig. 4d). Thus, bioassays using UZCA hydrotalcite concentrations of around 40 mg mL^{-1} of Zn-31.5 mg mL^{-1} of Cu allowed preventing the growth and fungal spore germination of *A. niger* (Table 4). The high antifungal activity of copper can be attributed to its oligodynamic characteristics and to the formation of small hydrotalcite particles providing, in one hand, a better interaction of the solid surface with microorganisms [10], and, on the other, to a faster release of ions to the fungal medium due to high specific surface area of these materials [18]. Furthermore, this high antifungal activity of copper compared to magnesium and zinc containing compounds can be attributed, in the case of bacteria but could also be considered for other microorganisms, to the following propositions/causes: (i) oxidative stress induction, (ii) membrane damage, (iii) particle internalization, and (iv) protein dysfunction and DNA transcriptional arrest [38]. Instead, magnesium or zinc may favor microorganism growth in small amounts [39].

4. Conclusions

Zn, Zn-Mg and Zn-Cu hydrotalcites showed an inhibitory effect on *A. niger* growth. In this study, the biocidal capacity depended mainly on the type of synthesis, the composition of the hydrotalcites and the concentrations used in microbiological tests. The biocidal characteristics of zinc and/or copper in conjunction with the alkalinity of these materials were favorable for preventing fungal spread. The ZnAl hydrotalcite, the more eco-friendly material of the analyzed series, showed a good biocide performance. The best antifungal behavior was observed for copper-containing hydrotalcite. The advantageous

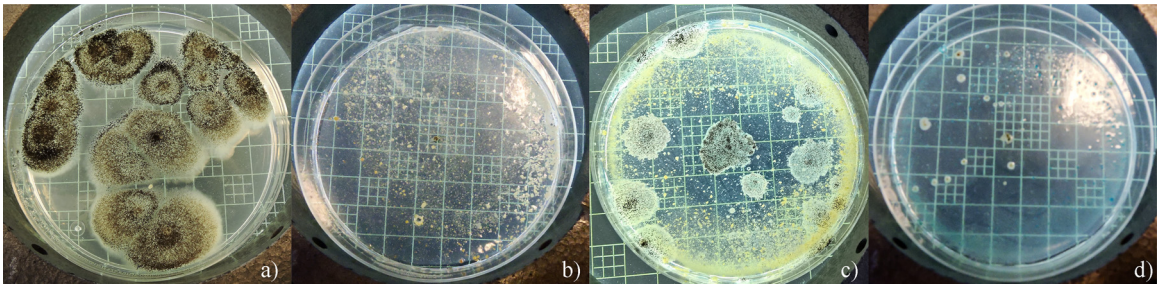

Fig. 4. *A. niger* growth for U series at 5 days. a) Control plate (without hydrotalcite). b) UZA sample containing: 80 mg of Zn. c) UZMA sample containing 120 mg of Zn-24.4 mg of Mg. d) UZCA sample containing 20 mg of Zn-15.2 mg of Cu.

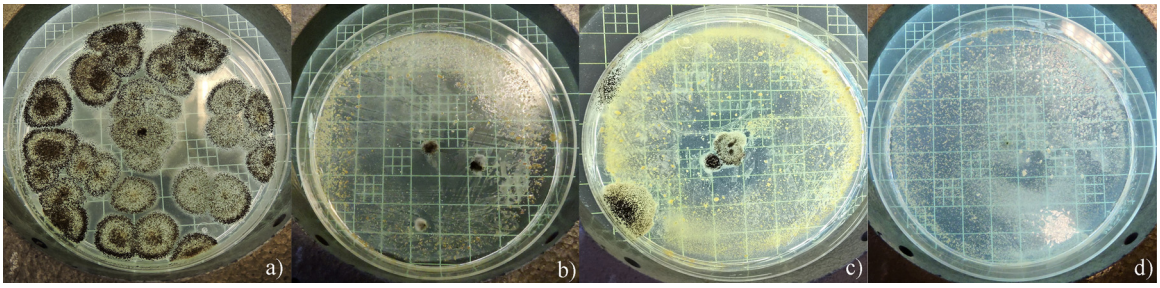

Fig. 5. *A. niger* growth for C hydrotalcites at 5 days. a) Control plate (without hydrotalcite). b) CZA containing 60 mg of Zn. c) CZMA containing 120 mg of Zn-17.6 mg of Mg. d) CZCA containing 20 mg of Zn-15.7 mg of Cu.

particularity of these anionic clays is based on the possibility of selecting the synthesis conditions for obtaining a product with predetermined properties. In this case, the tailoring of composition and synthesis conditions led to obtaining solids that contain biocidal cations fully dispersed into a nontoxic structure. Their excellent efficiency to inhibit fungal development in an environmentally friendly way makes these solids versatile materials that could fulfill specific technological requirements oriented to preventing the deleterious effects of microbiological contamination. The formulation of paints, where the materials obtained in this work could be incorporated to prevent fungal dissemination that causes damage to houses and buildings, affecting the human health, will be the object of further studies.

References

[1] A.K. Person, S.M. Chudgar, B.L. Norton, B.C. Tong, J.E. Stout, Aspergillus niger: an unusual cause of invasive pulmonary aspergillosis, J. Med. Microbiol. 59 (2010) 834–838, http://dx.doi.org/10.1099/jmm.0.018309-0.

[2] C.C. Gaylarde, L.H.G. Morton, K. Loh, M.A. Shirakawa, Biodeterioration of external architectural paint films – a review, Int. Biodeterior. Biodegrad. 65 (2011) 1189–1198, http://dx.doi.org/10.1016/j.ibiod.2011.09.005.

[3] P. Krijgsheld, R. Bleichrodt, G. van Veluw, F. Wang, W. Müller, J. Dijksterhuis, H. Wösten, Development in Aspergillus, Stud. Mycol. 74 (2013) 1–29, http://dx.doi.org/10.3114/sim0006.

[4] S. Campoy, J.L. Adrio, Biochem. Antifungals Pharmacol. 133 (2017) 86–96, http://dx.doi.org/10.1016/j.bcp.2016.11.019.

[5] N. Valette, T. Perrot, R. Sormani, E. Gelhaye, M. Morel-Rouhier, Antifungal activities of wood extractives, Fungal Biol. Rev. 31 (2017) 113–123, http://dx.doi.org/10.1016/j.fbr.2017.01.002.

[6] B. Gámiz, R. López-Cabeza, G. Facenda, P. Velarde, M.C. Hermosín, L. Cox, R. Celis, Effect of synthetic clay and biochar addition on dissipation and enantioselectivity of tebuconazole and metalaxyl in an agricultural soil: laboratory and field experiments, Agric. Ecosyst. Environ. 230 (2016) 32–41, http://dx.doi.org/10.1016/j.agee.2016.05.017.

[7] A. Megalathan, S. Kumarage, A. Dilhari, M.M. Weerasekera, S. Samarasinghe, N. Kottegoda, Natural curcuminoids encapsulated in layered double hydroxides: a novel antimicrobial nanohybrid, Chem. Cent. J. 10 (2016) 35, http://dx.doi.org/10.1186/s13065-016-0179-7.

[8] S.A.A. Moaty, A.A. Farghali, R. Khaled, Preparation, characterization and antimicrobial applications of Zn-Fe LDH against MRSA, Mater. Sci. Eng. C 68 (2016) 184–193, http://dx.doi.org/10.1016/j.msec.2016.05.110.

[9] J. Perera, M. Weerasekera, N. Kottegoda, Slow release anti-fungal skin formulations based on citric acid intercalated layered double hydroxides nanohybrids, Chem. Cent. J. 9 (2015) 27, http://dx.doi.org/10.1186/s13065-015-0106-3.

[10] G. Rocha-Oliveira, L.J. Dias-do Amaral, M. Giovanela, J. da Silva Crespo, G. Fetter, J.A. Rivera, A. Sampieri, P. Bosch, Bactericidal performance of chlorophyllin-copper hydrotalcite compounds, Water Air Soil Pollut. 226 (2015) 226–316, http://dx.doi.org/10.1007/s11270-015-2585-1.

[11] S.B. Vučetić, O.L. Rudić, S.L. Markov, O.J. Bera, A.M. Vidaković, A.S.S. Skapin, J.G. Ranogajec, Antifungal efficiency assessment of the TiO2 coating on façade paints, Environ. Sci. Pollut. Res. 21 (2014) 11228–11237, http://dx.doi.org/10.1007/s11356-014-3066-6.

[12] L. Yan-Yun, L. Song-Mei, L. Jian-Hua, Y. Mei, Preparation and anti-mildew Properties of TPN-SDS-layered double hydroxide nanohybrids, J. Inorg. Mater. 29 (2014) 515–522, http://dx.doi.org/10.3724/SP.J.1077.2014.13438.

[13] Y.-X. Zhang, S.-M. Li, J.-H. Liu, M. Yu, Preparation of BIT-layered double hydroxide and the study of antifungal properties, J. Inorg. Mater. 28 (2013) 1025–1032, http://dx.doi.org/10.3724/SP.J.1077.2013.12681.

[14] O. Şanli, N. Işiklan, Controlled release formulations of carbaryl based on copper alginate, barium alginate, and alginic acid beads, J. Appl. Polym. Sci. 102 (2006) 4245–4253, http://dx.doi.org/10.1002/app.24882.

[15] X. Qu, P.J.J. Alvarez, Q. Li, Applications of nanotechnology in water and wastewater treatment, Water Res. 47 (2013) 3931–3946, http://dx.doi.org/10.1016/j.watres.2012.09.058.

[16] A.M. Pereyra, M.R. Gonzalez, V.G. Rosato, E.I. Basaldella, A-type zeolite containing Ag+/Zn2+ as inorganic antifungal for waterborne coating formulations, Prog. Org. Coat. 77 (2014) 213–218, http://dx.doi.org/10.1016/j.porgcoat.2013.09.008.

[17] L. He, Y. Liu, A. Mustapha, M. Lin, Antifungal activity of zinc oxide nanoparticles against Botrytis cinerea and Penicillium expansum, Microbiol. Res. 166 (2011) 207–215, http://dx.doi.org/10.1016/j.micres.2010.03.003.

[18] M. Lobo-Sánchez, G. Nájera-Meléndez, G. Luna, V. Segura-Pérez, J.A. Rivera, G. Fetter, ZnAl layered double hydroxides impregnated with eucalyptus oil as efficient hybrid materials against multi-resistant bacteria, Appl. Clay Sci. 153 (2018) 61–69, http://dx.doi.org/10.1016/j.clay.2017.11.017.

[19] S. Sunayama, T. Sato, A. Kawamoto, A. Ohkubo, T. Suzuki, Disinfection effect of hydrotalcite compounds containing antimicrobial metals against microorganisms in water, Biocontrol Sci. 7 (2002) 75–81, http://dx.doi.org/10.4265/bio.7.75.

[20] C.E. Santo, N. Taudte, D.H. Nies, G. Grass, Contribution of copper ion resistance to survival of Escherichia coli on metallic copper surfaces, Appl. Environ. Microbiol. 74 (2008) 977–986, http://dx.doi.org/10.1128/AEM.01938-07.

[21] B. Wiyantoko, P. Kurniawati, T.E. Purbaningtias, I. Fatimah, Synthesis and characterization of hydrotalcite at different Mg/Al molar ratios, Procedia Chem. 17 (2015) 21–26, http://dx.doi.org/10.1016/j.proche.2015.12.115.

[22] F. Cavani, F. Trifirò, A. Vaccari, Hydrotalcite-type anionic clays: preparation, properties and applications, Catal. Today 11 (1991) 173–301, http://dx.doi.org/10.1016/0920-5861(91)80068-K.

[23] W. Cai, J. Yu, S. Gu, M. Jaroniec, Facile hydrothermal synthesis of hierarchical boehmite: sulfate-mediated transformation from nanoflakes to hollow microspheres, Cryst. Growth Des. 10 (2010) 3977–3982, http://dx.doi.org/10.1021/cg100544w.

[24] G.V. Rosato, R. Lofeudo, Patologías en muros de construcciones históricas ocasionadas por vegetación invasiva, VI Congr. Int. Sobre Patol. Y Recuper. Estructuras, (2010) Córdoba, Argentina www.edutecne.utn.edu.ar/cinpar_2010/Topico4/CINPAR003.pdf.

[25] A. Sommer, A. Romero, G. Fetter, E. Palomares, P. Bosch, Exploring and tuning the anchorage of chlorophyllin molecules on anionic clays, Catal. Today 212 (2013) 186–193, http://dx.doi.org/10.1016/j.cattod.2013.03.014.

[26] X. Xie, X. Ren, J. Li, X. Hu, Z. Wang, Preparation of small particle sized ZnAl-hydrotalcite-like compounds by ultrasonic crystallization, J. Nat. Gas Chem. 15 (2006) 100–104, http://dx.doi.org/10.1016/S1003-9953(06)60015-7.

[27] O. Bergadà, I. Vicente, P. Salagre, Y. Cesteros, F. Medina, J.E. Sueiras, Microwave effect during aging on the porosity and basic properties of hydrotalcites, Microporous Mesoporous Mater. 101 (2007) 363–373, http://dx.doi.org/10.1016/j.micromeso.2006.11.033.

[28] J. Liu, P. Yao, Z.-M. Ni, Y. Li, W. Shi, Jahn-Teller effect of Cu-Mg-Al layered double hydroxides, Acta Physico-Chim. Sin. 27 (2011) 2088–2094, http://dx.doi.org/10.3866/PKU.WHXB20110923.

[29] A. Vaccari, Clays and catalysis. A promising future, Appl. Clay Sci. 14 (1999) 161–198, http://dx.doi.org/10.1016/S0169-1317(98)00058-1.

[30] U. Costantino, F. Marmottini, M. Sisani, T. Montanari, G. Ramis, G. Busca, M. Turco, G. Bagnasco, Cu-Zn-Al hydrotalcites as precursors of catalysts for the production of hydrogen from methanol, Solid State Ion. 176 (2005) 2917–2922, http://dx.doi.org/10.1016/j.ssi.2005.09.051.

[31] S.N. Britvin, Structural diversity of layered double hydroxides, In: Miner. as Adv. Mater. I, Krivovichev S.V., Berlin, Heidelberg, 2008: pp. 123–128. 10.1007/978-3-540-77123-4_17.

[32] G. Carja, G. Ciobanu, M. Toyota, The role of the organic solvent in obtaining hydrotalcite-like anionic clay nanopowders with specific textural and porous properties, Sci. Study Res. – Chem. Chem. Eng. Biotechnol. Food Ind. VII (2006) 157–162 http://pubs.ub.ro/?pg=revues&rev=cscc6&num=200607&vol=1&aid=1075.

[33] M.J. dos Reis, F. Silvério, J. Tronto, J.B. Valim, Effects of pH, temperature, and ionic strength on adsorption of sodium dodecylbenzenesulfonate into Mg-Al-CO3 layered double hydroxides, J. Phys. Chem. Solids 65 (2004) 487–492, http://dx.doi.org/10.1016/j.jpcs.2003.09.020.

[34] M. Wei, J. Wang, J. He, D.G. Evans, X. Duan, In situ FT-IR, in situ HT-XRD and TPDE study of thermal decomposition of sulfated β-cyclodextrin intercalated in layered double hydroxides, Microporous Mesoporous Mater. 78 (2005) 53–61, http://dx.doi.org/10.1016/j.micromeso.2004.09.016.

[35] L. Cocheci, P. Barvinschi, R. Pode, E. Popovici, E.M. Seftel, Structural characterization of some Mg/Zn-Al type hydrotalcites prepared for chromate sorption from

wastewater, Chem. Bull. Politehnica Univ. Timisoara 55 (2010) 40–45 http://chemicalbulletin.ro/Chemical-Bulletin-Article_XXwQm.html.
[36] S.S. Santos, J. a M. Corrêa, Síntese de hidróxidos duplos lamelares do sistema Cu, Zn, Al-CO3: propriedades morfológicas, estruturais e comportamento térmico, Ceramica 57 (2011) 274–280, http://dx.doi.org/10.1590/S0366-69132011000300004.
[37] A.M. Torres López, J.C. Quintero Díaz, L. Atehortua Garcés, Efecto de nutrientes sobre la producción de biomasa del hongo medicinal Ganoderma lucidum, Rev. Colomb. Biotecnol. 13 (2011) 103–109 http://www.scielo.org.co/scielo.php?script=sci_arttext&pid=S0123-34752011000100014&lng=en&tlng=es.
[38] P. Nagarajan, P.K.K. Samantaray, L. Das, G. Madras, S. Bose, Selective cleavage of polyphosphoester in crosslinked copper based nanogels: enhanced antibacterial performance through controlled release of copper, Nanoscale (2017) 12664–12676, http://dx.doi.org/10.1039/C7NR02446K.
[39] A. Matheson, M.C.M. Kwong, R. Cheung, Influences of environmental ionic strength pH, and magnesium ion on bactericidal and lytic activities of p-lysin on Bacillus subtilisl Eflects of Ionic Strength and pH orz Bactericidal Lytic Studies with Cells and Protoplasts, Can. J. Microbiol. 18 (1972) 1–6.